Journal of
Composites Science

MDPI

Supplementary Materials: 3D X-Ray Microscopy as a Tool for in Depth Analysis of the Interfacial Interaction between a Single Carbon Fiber and an Epoxy Matrix after Mechanical Loading

Julia Vogtmann [1], Andreas Klingler [2], Thomas Rief [3] and Martin Gurka [1,*]

S1 Micromechanical description of stress state according to Broutman [1]:

$$\sigma_n = \frac{\sigma_z(\vartheta_m - \vartheta_f)E_f}{(1+\vartheta_m)E_f + (1-\vartheta_f-2\vartheta_f^2)E_m} \quad \textbf{(Eq.1)}$$

To describe the stress normal to the fiber-matrix interface σ_n within the Broutman test specimen [1,2], caused by axial, compressive stresses (z-direction) σ_z, under consideration of the different Poisson ratios of the polymeric matrix ϑ_m and the fiber ϑ_f, the Broutman equation is used. Where E_m and E_f are the Young´s moduli of the matrix and the fiber, respectively. A combination of prevailing failure modes after the test (cohesive fiber failure and adhesive fiber-matrix interphase failure) has already been observed by other authors. [2,3] [2] assumed a correlation between high interphase strength and cohesive fiber failure due to higher compression stresses, than compression strength of the fiber. A stop restart mechanism was observed for the specimens where debonding could be observed. Also, in [4] the Broutman test was applied to perform a compression fragmentation test and compare with the results of the standard tensile fragmentation test to determine the shear stress in the interface. For interpretation of this compressive fragmentation test the critical fiber length has to be calculated. The critical fiber length is an important parameter, it describes the length of the fiber at which more energy would have to be expended for debonding and sliding than for fiber failure. The usual calculation of this length according to Kelly and Tyson [5] is difficult to, as the stress level at the separate fragment ends is not zero, since the fragments remain in contact after fracture. This suggests a high stress discontinuity at the failure points, thus making the stress state very difficult to describe. The description of such micromechanical processes is often very difficult, also due to the lack of information on the damage itself.

S2 Failure mechanism during Broutman test analyzed with additional methods

To understand the interphase failure mechanism, a progressive loading test was done. Different loading steps were analyzed with the polarized light microscope indicating that fiber failure and debonding occur simultaneously.

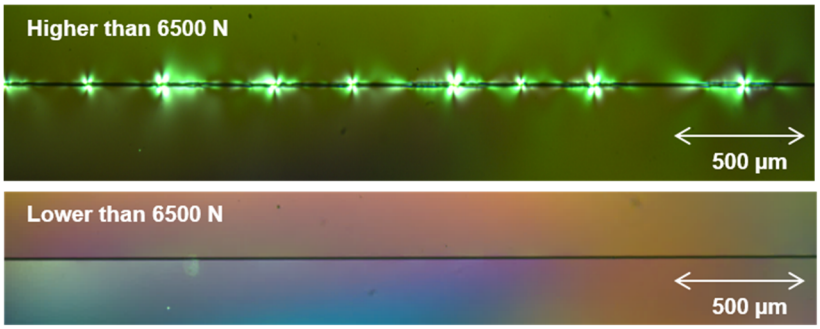

Figure S 1. post mortem polarized light microscopy images of the same Broutman test specimens (non-toughened) taken after different loading steps (4000 N and 6000 N).

S3 illustration of the cum. Number of AE events (class 1) over the applied load of all tested specimens

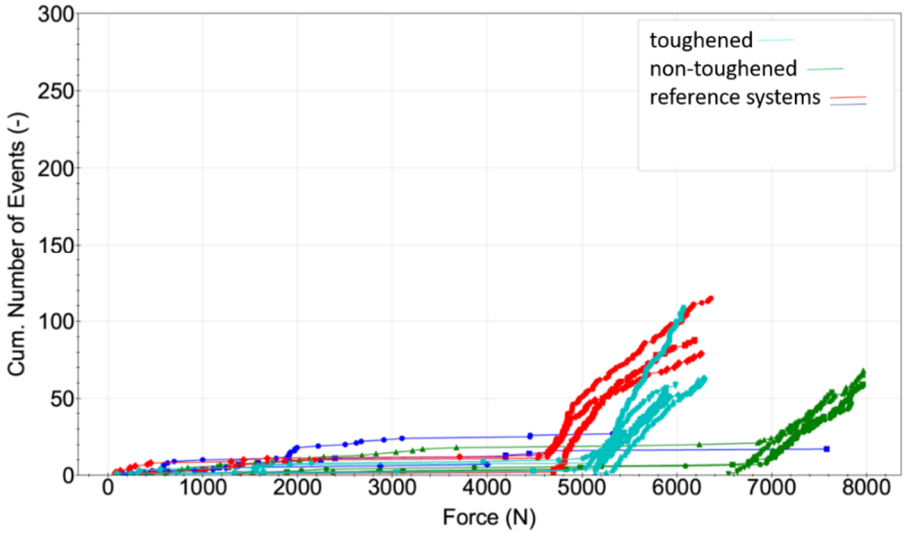

Figure S 2. shows the cumulative number of Events of class 1, which describes a class of AE events which can be correlated (frequency dependent) with the fiber and the compression force applied in N for the toughened system, the non-toughened and two different reference systems. The further results of the tested systems and the test itself will be published elsewhere.

Figure S3 polarized light microscopy images of the toughened and non-toughened matrix system after loading

S3 supporting information about the Broutman test configurations and the test set-up

Broutman test was done using AE as control device to determine the debonding stress. Five samples of each configuration were tested. All samples were analyszed visually with polarized light microscopy revealing a repoducible failure pattern. A reference configuration without any fiber (not shown in **Figure S 2**) was used to distinguish between AE signals gathered from the matrix- and the C-fiber-dependent signals (frequency-dependent). The Broutman test itself and the description of the interpretation of the AE data will be published elsewhere. A brief description can be found in [6]. The frequency dependence of failure mechanisms in composites analyszed with AE is presented in [7].

S4 Comparison between toughened and non-toughened matrix systems via polarized light microscopy

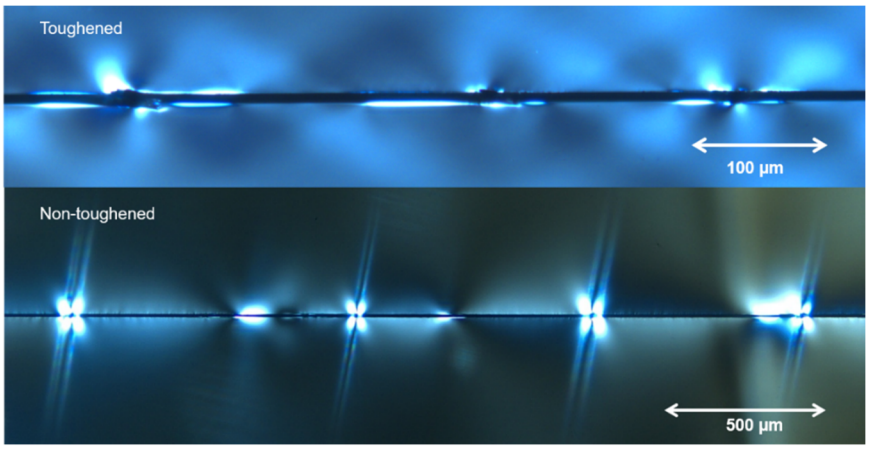

Figure S 3. post mortem polarized light microscopy image of the toughened and the non-toughened matrix system, indicating no visible difference in the degree of fracture.

References

1. Broutman, L.J. Glass-Resin Joint Strength and Their Effect on Failure Mechanisms in Reinforced Plastics. *Polym. Eng. Sci.* **1966**, *6*, 263–272, doi:10.1002/pen.760060316.
2. Ageorges, C.; Friedrich, K.; Schüller, T.; Lauke, B. Single-Fibre Broutman Test: Fibre–Matrix Interface Transverse Debonding. *Composites Part A: Applied Science and Manufacturing* **1999**, *30*, 1423–1434, doi:10.1016/S1359-835X(99)00045-7.
3. Schüller, T.; Beckert, W.; Lauke, B.; Ageorges, C.; Friedrich, K. Single Fibre Transverse Debonding: Stress Analysis of the Broutman Test. *Composites Part A: Applied Science and Manufacturing* **2000**, *31*, 661–670, doi:10.1016/S1359-835X(00)00034-8.
4. Ageorges, C. Experiments to Relate Carbon-Fibre Surface Treatments to Composite Mechanical Properties. *Composites Science and Technology* **1999**, *59*, 2101–2113, doi:10.1016/S0266-3538(99)00067-6.
5. Kelly, A.; Tyson, W.R. Tensile Properties of Fibre-Reinforced Metals: Copper/Tungsten and Copper/Molybdenum. *Journal of the Mechanics and Physics of Solids* **1965**, *13*, 329–350, doi:10.1016/0022-5096(65)90035-9.
6. 22nd Symposium on Composites | Book | Scientific.Net Available online: https://www.scientific.net/book/22nd-symposium-on-composites/978-3-0357-3453-9 (accessed on 29 March 2021).
7. Kelkel, B.; Popow, V.; Gurka, M. *Inline Quantification and Localization of Transverse Matrix Cracking in Cross-Ply CFRP during Quasi-Static Tensile Testing by a Joint Event-Based Evaluation of Acoustic Emission and Passive IR Thermography*; Vol. 2019;.